[45]rf pickup reduced the galvanometer sensitivity somewhat.
[46]M. J. Stephen, Phys. Rev. 186, 393 (1969).
[47]A factor of π was omitted from the expression for i_N in II.
[48]A. J. Dahm, A. Denenstein, D. N. Langenberg, W. H. Parker, D. Rogovin, and D. J. Scalapino, Phys. Rev. Letters 22, 1416 (1969).
[49]H. Kanter and F. L. Vernon, Jr., Phys. Rev. Letters 25, 588 (1970).
[50]W. H. Parker, D. N. Langenberg, A. Denenstein, and B. N. Taylor, Phys. Rev. 177, 639 (1969). For a review and further references, see J. Clarke, Am. J. Phys. 38, 1071 (1970).
[51]B. N. Taylor, W. H. Parker, D. N. Langenberg, and A. Denenstein, Metrologia 3, 89 (1967).

PHYSICAL REVIEW B VOLUME 4, NUMBER 9 1 NOVEMBER 1971

Study of Supercooling and Thermal Conductivity in Superconducting Molybdenum†

A. Waleh and N. H. Zebouni
Department of Physics and Astronomy, Louisiana State University, Baton Rouge, Louisiana 70803
(Received 10 June 1971)

The critical magnetic field and the associated supercooling are measured and analyzed in superconducting molybdenum. The coexistence of a superconducting surface sheath with a supercooled normal bulk is confirmed. Thermal-conductivity measurements are analyzed and the possible influence of s-d scattering close to T_c is discussed.

I. INTRODUCTION

Superconductivity in the transition metals has been the subject of many experimental and theoretical investigations in recent years. Many of the experiments and observations on this group of elements, in particular, studies of the absence or considerable reduction of the isotope effect,[1] the pressure dependence of the transition temperature T_c,[2] the relation of T_c to the total density of states at the Fermi surface,[3] the effect of magnetic impurities,[4] and the empirical rules relating T_c to the position in the Periodic Table,[5] have led some of the investigators[6] to suggest mechanisms different from the electron-phonon interaction, as originally proposed by Bardeen *et al.*[7] (BCS), to be partially responsible for superconductivity in the transition metals. On the theoretical side, however, in the spirit of a two-band model for the electronic structure of the transition metals[8] and assuming the Fermi surface separable into s- and d-like regions, it has been shown by Garland[9] that experimentally observed superconducting properties of the transition metals could be explained by a single-gap theory appropriate to dirty[10] materials. Based on his model and the single-gap theory, Garland[11] has carried out calculations of the isotope effect coefficients in the limit of sufficient dirtiness[12] and has shown that the experimental evidence supports the BCS theory and the idea of phonon-induced superconductivity. Although the superconducting state parameters have been calculated[13] using the electron-phonon interaction and were found to be in agreement with the experimental results, the present knowledge of the electronic-band structure of the transition metals is insufficient to resolve the controversy and completely justify the theoretical models.

Much of the success of the experiments on transition metals is due to the recent purification techniques. In fact, elements such as molybdenum can be sufficiently pure to show the characteristics of a "clean" superconductor.[9,10] Thus, it seems of interest to carry out further experimental investigations of the superconducting transition and of the transport properties of molybdenum, particularly below 1 °K where molybdenum becomes superconducting. In this temperature region, for a pure metal, one can safely assume that the heat conductivity is predominantly electronic. Also, since molybdenum has a very high Debye temperature relative to its superconducting transition temperature and because of a large electronic mean free path due to its high purity, one may expect the scattering of the electrons by thermally excited lattice vibrations to be negligible as compared to their elastic scattering by static imperfections such as impurities, lattice defects, or, at even lower temperatures, by the boundaries. In turn, in a very pure transition metal one can hope to see some influence of another scattering process: the electron-electron scattering or s-d scattering. Under these conditions, the study of the thermal conductivity of molybdenum in the normal and superconducting states will prove very useful for comparison with the theory of Bardeen, Rickayzen, and Te-

word[14] (BRT) and for the determination of the possible contributions arising from the s-d interaction.[8,15]

Superconductivity in molybdenum was first reported by Geballe *et al.*[16] Since then, measurements have been made of the isotope effect,[1] the ultrasonic attenuation,[17,18] the critical magnetic field,[19,20] the specific heat,[21] and the magnetization[22] of this element. In this work, we present the measurements of the critical field and supercooling as well as those of the thermal conductivity in the superconducting and normal states on single crystals of molybdenum.

In Secs. II and III, the pertinent details of the apparatus and the experimental procedure are briefly reviewed. Section IV is devoted to the presentation and discussion of the results. Finally, in Sec. V the conclusion of this study is presented.

II. APPARATUS

A. Cryostat

Below 1 °K, a He^3 refrigerator similar to the one described by Reich and Garwin[23] was used. The cryostat could be operated in two modes: continuous operation with the lowest temperature of 0.7 °K and batch operation with the lowest temperature of 0.33 °K. The temperature regulation was maintained by an electronic heater feedback system[24] developed for the thermal conductivity measurements that was capable of maintaining the temperature constant within better than 1 mdeg over a 30-min period.

B. Magnetic Field

The external applied field was provided by a superconducting solenoid, 7 in. long and $1\frac{1}{2}$ in. in diam, wound with Nb-Ti wire[25] on a stainless-steel core tightly fitted around the vacuum chamber surrounding the sample. The solenoid was calibrated by means of a Hall probe against a precision regulated magnet. The characteristic calibration at the center of the solenoid was 420.5 G/A. Since the sample used for critical field measurements was only 1 in. long, the field was considered to be homogenous over the volume of the sample within a fraction of a percent and no end corrections were made.

For the thermal measurements which were carried out on a 3-in.-long sample, the above solenoid was replaced by another one of comparable dimensions but with end corrections to keep the field homogenous within $1\frac{1}{2}$ in. from the center of the solenoid. The characteristic calibration at the center of the solenoid was 230 G/A.

C. Thermometry

In the He^3 cryostat, secondary thermometers (Allen-Bradley resistors) were calibrated against the vapor pressure of the He^3 bath. The best conditions for the calibration were obtained by pumping the system to the lowest temperature attainable, then shutting off the He^3 system completely from the outside. The system then warmed up slowly over a period of 2–3 h, during which the calibration of the thermometers versus the slowly rising vapor pressure was carried out. The instrument used to measure the vapor pressure of the He^3 was a type-I quartz Bourdon tube manufactured by Texas Instruments, Inc. The tube range was 0–200 Torr, and its sensitivity was about 1% in the 10^{-2}-Torr region and 0.1% in the 1-Torr region. At the lowest temperatures, a correction to the pressure reading was made[26] in order to take into account the thermomolecular effect. The thermometer current was limited to less than 0.25 μA in order to avoid self-heating.

For the temperature dependence of the critical field measurements, a 10-Ω $\frac{1}{10}$-W Allen-Bradley resistor, which was previously calibrated by Blewer *et al.*,[27] was calibrated again following the procedure stated above and the calibration curve was found to be reproducible. Subsequently, the temperatures were obtained from the calibration of this thermometer.

For the thermal-conductivity measurements, new thermometers (with no previous calibration) had to be used, and because of the necessary modifications introduced in the He^3 system, the calibration of the thermometers was carried out in the following manner: A 10- and 30-Ω $\frac{1}{10}$-W Allen-Bradley resistor were calibrated against He^3 vapor pressure in the temperature ranges of 0.3–0.9 °K and 0.8–1.1 °K, respectively. The calibrations were repeated several times to ensure reproducibility of the results. The thermometers were found to obey, quite accurately, a relation between their resistance R and the vapor pressure p of the He^3 liquid given by[28] $\log_{10}R = a + \sum_n b_n (\log_{10}P)^n$, with n being equal to 6 and 5, respectively. This relation is linear over the upper temperatures of either range and this linearity was utilized for further correction in the calibration as follows: The 30-Ω thermometer was calibrated against the vapor pressure of He^4 and the result was converted to a relation between $\log_{10}R$ and $\log_{10}P$, where P is the He^3 vapor pressure corresponding to the given He^4 vapor pressures. The two calibrations were plotted together and the He^3 calibration was shifted along the $\log_{10}P$ axis to match the continuity of the two straight lines. The shift was assumed to be the same at all temperatures of the He^3 calibration and new temperatures were calculated accordingly. The correction to the He^3 calibration was about 5 mdeg at the lowest attainable temperature and about 15 mdeg at 0.9 °K. This correction was accounted for by assuming a systematic error due to the nonideal

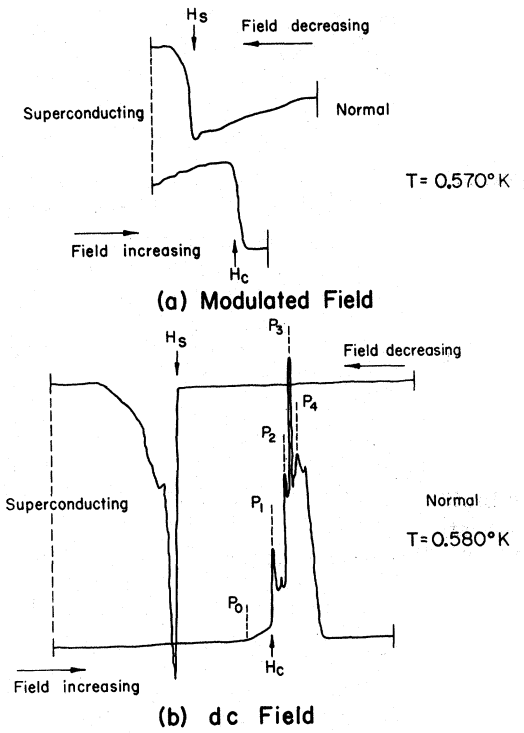

FIG. 1. Typical recordings of N-S and S-N transition on x-y recorder. (a) is the induced emf observed through a lock-in amplifier; (b) is the induced emf observed directly after amplification. The individual peaks are distinct and reproducible and p_1 is identified with H_c.

conditions prevailing in the measurement of the vapor pressure of He^3.

The temperatures between 1.1–4.2 °K were determined from the calibration of two 50-Ω $\frac{1}{10}$-W Allen-Bradley resistors calibrated against the vapor pressure of He^4.

III. EXPERIMENTAL PROCEDURE

A. Critical Field Measurements

The sample used for these measurements was a triple electron-beam-zone-refined single crystal in the form of a rod 1 in. long and $\frac{1}{8}$ in. diam purchased from Materials Research Corp. The resistance ratio of the sample was measured and found to be $R_{300}/R_{1.2} \simeq 10^4$ with the residual resistivity $\rho_0 = 5.7\times10^{-10}$ Ω cm. From the measurement of ρ_0, the mean free path was estimated by using the relation $l = V_F\tau = 3\sigma/2e^2N(0)\,V_F$, where σ is the residual electrical conductivity, V_F is the Fermi velocity, and the density of states is $N(0) = 3\gamma/2\pi^2k^2$. Deducing the electronic specific heat constant γ, the Fermi velocity V_F, and the coherence length ξ_0 from our critical field measurements yields $l \simeq 2.8\times10^{-2}$ cm and its ratio to the coherence length ξ_0, $l/\xi_0 \simeq 780$.

The transition at a given temperature was detected by observing the emf induced in a pickup coil wound around the sample, as an axial external field was swept linearly at a rate of about 0.25 G/sec through the value of the critical field. The emf was used to drive the y axis of a x-y recorder, the x axis of which was driven by a voltage proportional to the current in the solenoid. Two methods were used to observe the emf. In the first method, hereafter referred to as modulated-field technique, the external dc field was modulated by a 270-cycle field and the emf induced in the coil was fed to a lock-in amplifier, the output of which was connected to the y axis of the recorder. Though the detection of the transition was accurate, as shown in Fig. 1(a), the method failed to reveal the details of the transition. An alternative method, in which there was no modulation superimposed on the external field, hereafter referred to as dc field technique, was to observe the emf directly after amplification by a dc amplifier. This method proved satisfactory in producing the details of the transition in a manner similar to that observed in other measurements.[21,22] In Fig. 1(b), a typical transition signal is shown. The sample was first cooled down to the lowest temperature in zero field. The field was then linearly increased and the external field at the transition to the normal state was identified with the thermodynamic critical field H_c. The direction of the field sweep was then reversed until the completion of the normal to superconducting transition, and the value of the external field at which the transition started was identified with the supercooling field H_s. The sample was brought to the normal state again by increasing the field and the value of H_c was observed to be reproducible. The bath temperature was then raised to a higher value, and the values of H_s and H_c at the new temperature were, respectively, determined by a downward sweep followed by an upward sweep of the external field such that the final state of the sample was normal. The bath temperature was then raised further and the procedure was repeated until the transition temperature T_c was reached.

B. Thermal Measurements

The sample used for the thermal measurements was 3 in. long and had original characteristics similar to the first sample. This sample was first reduced to a rectangular cross section of approximately 1×1 mm by grinding with Carborundum powder and polishing with emery paper No. 600. It was then annealed at about 1200 °C and 10^{-5} Torr for 16 h. The surface oxidation and the local strains close to the surface were removed in a strong acid solution (H_2SO_4, HNO_3, HF, and H_2O_2) and finally the sample was etched several times in a strong etchant (HCl and H_2O_2). The final average cross section of the sample was approxi-

mately $\frac{1}{3}\times\frac{2}{3}$ mm. The electrical resistance stayed constant between 4.2 and 1 °K with a resistance ratio of $\Gamma = R_{300}/R_{1.2} = 3500$ and a residual resistivity ρ_0 of 15.8×10^{-10} Ω cm. The resistance ratio was smaller than that of the first sample suggesting a higher concentration of structural defects and probably incomplete annealing. Using V_F, γ, and ξ_0 of the first sample, the electronic mean free path was estimated to be $l \simeq 1.0\times10^{-2}$ cm with the ratio $l/\xi_0 = 285$, indicating the high purity of the sample. The sample, inside a vacuum calorimeter, was soldered to the He^3 copper cup. A heater of Constantan wire No. 40 was wound at the end of the sample and covered with General Electric No. 7031 glue. The temperature gradient along the sample was measured by two carbon resistance thermometers whose copper windings were soldered to copper spots welded on the sample. The temperature measuring circuit and the method of measuring thermal gradient in the He^4 range of temperature have been described by Wasim and Zebouni.[29] A similar method was followed in the He^3 range of temperature. The two thermometers at the two ends of the sample were electrically connected as two arms of a bridge which was initially balanced at a bath temperature T_0 in the absence of any heat flow through the sample. The temperature of the bath was then lowered to $T_0 - \Delta T$, where ΔT was of the order of 30–50 m °K. Then the heat current was adjusted so that the thermometer closest to the heat source had the same resistance as at T_0. The resistance of the calibrated thermometer, placed at the cold end of the sample, would then correspond to $T_0 - \delta T$, where δT is the temperature drop along the sample and, therefore, the temperature gradient is obtained directly from the characteristics of only one thermometer.

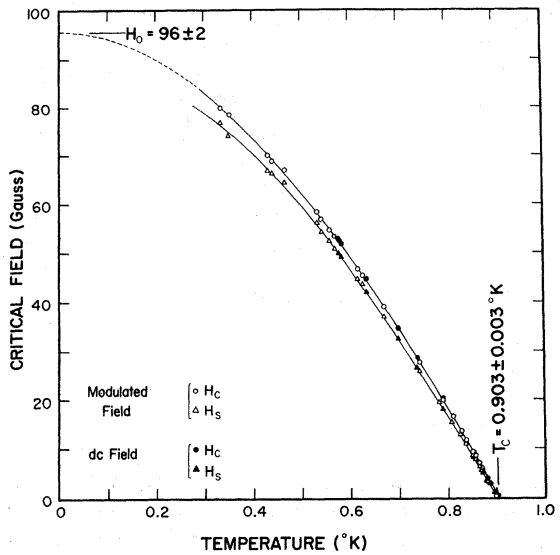

FIG. 2. Temperature dependence of the thermodynamic critical field H_c and the supercooling field H_s of molybdenum. The solid curves are least-squares fits of the form $H = H_0 + \Sigma_{n=1}^{3} a_n T^{2n}$ to the experimental data of the modulated-field technique (see Ref. 30).

IV. RESULTS AND DISCUSSION

A. Critical Fields

The temperature dependences of the thermodynamic critical field H_c and the supercooling field H_s are plotted in Fig. 2 for the two techniques. The solid lines are least-squares fits of the form[30] $H = H_0 + \sum_n a_n T^{2n}$ to the data from the modulated-field technique. The values $H_c(0) = 96 \pm 2$ and $T_c = 0.903 \pm 0.003$ are calculated from the expression corresponding to the upper curve at the two limits $T = 0$ and $H = 0$, respectively. The data from the modulated-field technique were used for the least-squares fit because they extend to lower temperatures than the dc field data. The latter, however, proved more useful in producing the details of the transition signal. It was observed that the normal-to-superconducting transition is very sharp while the superconducting-to-normal transition has distinct individual peaks.[21,22] These peaks show complete reproducibility at all temperatures, although they smear out into one smooth peak close to T_c. Figure 1(b) shows a typical transition signal from the dc field technique, and the individual peaks are clearly distinguished. The onset P_0 of the transition was attributed to the end effects, and the first peak P_1 was taken to represent the penetration of the external field into the bulk of the sample, i.e., H_c. For the completeness of the comparison of the two techniques, however, the values of the external field at P_4 are plotted in Fig. 2 and those at P_1 are plotted in Fig. 3. With the exception of Fig. 2, H_c is to correspond to the peak P_1 throughout the present work. Figure 3 is the plot of H_c vs $(T/T_c)^2$. We have also plotted the values of the critical field computed by Rorer *et al.*[21] from their specific-heat data. Their Mo-4 sample was chosen for comparison because its characteristics seemed closer to ours (same commercial source). With the exception of the value for the transition temperature T_c, the over-all agreement of the results is excellent. The values of the electronic specific-heat constant and the energy-gap parameter at $T = 0$ were obtained from the expressions of BCS, $\gamma = 1/19.4\,(dH_c/dT)^2_{T=T_c}$ and $2\epsilon(0)/kT_c = (4\pi/\sqrt{3})\,[H_c^2(0)/8\pi\gamma T_c^2]^{1/2}$, using the experimental values of T_c and $(dH_c/dT)_{T=T_c}$ and $H_c(0)$. As shown in Table I, they are in good agreement with those of the specific-heat measurements. In Table I, some of the results of this work are presented and compared with other experiments and available calculations. To complete the comparison, the deviation of the

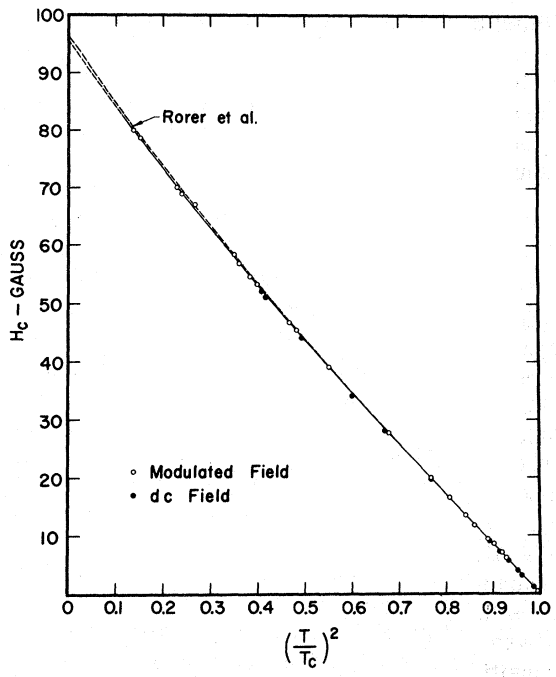

FIG. 3. Thermodynamic critical field of molybdenum. The dashed curve is that computed by Rorer *et al.* from their specific-heat measurements.

critical field of molybdenum from a simple parabolic law, together with the results of BCS[7,31] in the limit of weak coupling, are shown in Fig. 4. The deviation is found to be similar to that predicted by the BCS theory.

Supercooling. The temperature dependence of the supercooling field H_s in molybdenum was shown in Fig. 2. It is observed that H_s, at which the transition to the Meissner state takes place, is always smaller than H_c at all temperatures. The significance of H_s is in its relation with the surface nucleation field H_{c3} and its distinction from the bulk nucleation field H_{c2} in a type-I superconductor. Here both H_{c3} and H_{c2} have to be given special meanings. Saint-James and de Gennes (SJdG),[32] using the Ginzburg-Landau[33] equation, have shown that in a magnetic field parallel to the sample surface, a localized superconducting region can be present near the surface (surface sheath) up to a field H_{c3}, significantly higher than H_{c2}, with $H_{c3}/H_{c2} = 1.695$ at $T = T_c$. Recent calculations[34–36] of H_{c3}/H_{c2} show that this ratio increases as the temperature is lowered below T_c. In type-I superconductors, H_{c2} is smaller than H_c and, depending on the Ginzburg-Landau parameter, H_{c3} may be smaller also. Nevertheless, both critical fields still have significance.[34] H_{c2} is the smallest field for which the sample can be kept metastably normal in a "supercooling" situation (when surface effects are not important) and H_{c3} is the smallest field for which the sample can be kept metastably normal in a "supercooling" situation when the field is parallel to the surface. SJdG were first to suggest that in type-I superconductors, when the field is parallel to the surface, the supercooling field is H_{c3} (whenever $H_{c3} < H_c$) rather than H_{c2}. However, from the one-dimensional Ginzburg-Landau equations, Feder[37] has predicted the existence of a metastable superconducting surface sheath on a supercooled material, even when $H_{c3} < H_c$, if the Ginzburg-Landau parameter κ is larger than a critical value κ_c. Thus, it is only when $\kappa < \kappa_c$ that H_{c3} can be identified with the supercooling field. The limiting field, below which there are no surface solutions (the field at which transition to the Meissner state takes place), has been calculated by Park[38] who has shown that there are metastable surface solutions below H_c even when $H_{c3} > H_c$. The magnetization experiments of McEvoy *et al.*[39] on lead and tantalum have shown a qualitative agree-

TABLE I. Comparison of experimental results on superconducting molybdenum.

Technique	T_c (°K)	$-\frac{dH_c}{dT}\Big\vert_{T_c}\left(\frac{G}{°K}\right)$	$H(0)$ (G)	$\frac{2\epsilon(0)}{kT_c}$	$\gamma\left(\frac{mJ}{mole\ deg^2}\right)$
Critical magnetic field[a]	0.930		98.2		1.61
Critical magnetic field[b]	0.916	~188	86±1.5		
Specific heat[c]	0.917	178±2	96±3	3.40± 0.10	1.87±0.02
Magnetization[d]	0.903		98		
Ultrasonic attenuation[e]	0.92±0.01		114	3.5±0.2 ($\vec{q} \parallel$ [100])	
Ultrasonic attenuation[f]	0.92±0.01			3.3±0.2 ($\vec{q} \parallel$ [100])	
				3.5±0.2 ($\vec{q} \parallel$ [110])	
				3.1±0.2 ($\vec{q} \parallel$ [111])	
Present work:					
Critical magnetic field	0.903±0.003	187±3	96±2	3.40±0.1	1.80±0.06
Thermal conductivity	0.903±0.003			3.2 ±0.1	

[a]See Ref. 19.
[b]See Ref. 20.
[c]See Ref. 21.
[d]See Ref. 22.
[e]See Ref. 17.
[f]See Ref. 18.

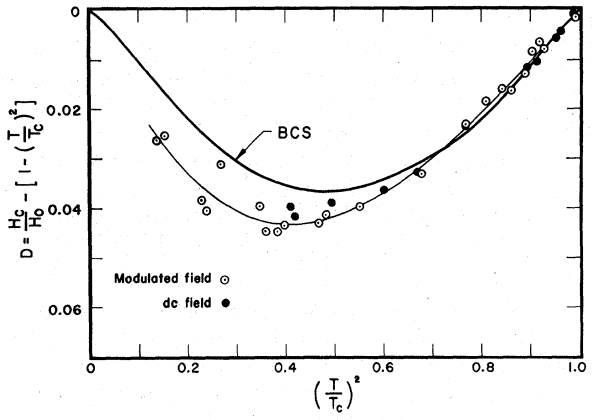

FIG. 4. Deviation of the critical field of molybdenum from that of a simple parabolic law. The dark solid line is the corresponding deviation of the BCS theory for superconducting with weak coupling.

ment with the above theoretical predictions. The reported values of κ_c from the theories and from experiment range from 0.406 to 0.409.

Since it is apparent that H_{c3} cannot be identified with H_s over the whole range of temperature and a direct measurement of H_{c3} was not possible in the present experiment, it is our purpose to compare the experimental values of H_s with the theoretical calculations[34,35] of H_{c3}. This comparison is more meaningful if made as a function of the Ginzburg-Landau parameter κ rather than as a function of temperature. The temperature dependence of κ can be determined from the ratio $H_{c2}(t)/H_c(t)$, but $H_{c2}(t)$ cannot be observed without difficulty in type-I superconductors. Fortunately, the theoretical computations of κ and H_{c2} can be made with a fairly high degree of confidence. Using a gauge-invariant solution of the linearized Gor'kov[40] equations, Helfand and Werthamer[41] have calculated the bulk nucleation critical field H_{c2} and the Ginzburg-Landau parameter κ for all impurity concentrations and all temperatures below T_c. Their impurity concentration parameter $\lambda = 0.882\,\xi_0/l$ is estimated to be of the order of 10^{-3} for our sample, thus putting the molybdenum well within the pure limit of their theory. From their calculations, $\kappa(\lambda, t) = \kappa(\lambda, T_c) f(\lambda, t)$, where $t = T/T_c$ and $f(t, \lambda)$ is a normalized known function of the reduced temperature and the parameter λ. Therefore, one can determine $\kappa(t)$ if the value of κ at the transition temperature is known. From the preliminary analysis of the data, it was predicted that $\kappa(T_c) < \kappa_c$ and, therefore, in the region close to T_c, $H_{c3} = H_s$. Then, assuming the validity of SJdG's relation,[32] $\kappa(T_c)$ can be obtained from the extrapolation of the experimental values of the ratio $H_{c3}/1.695\sqrt{2}H_c$ to $T = T_c$, which yields $\kappa(T_c) = 0.365 \pm 0.005$. From $\kappa(t)$ and the relation $H_{c2}(t) = \kappa(t) H_c(t)$, one can determine $H_{c2}(t)$ using the experimental temperature dependence of $H_c(t)$. The calculated values of $H_{c2}(t)$ are shown in Fig. 5 together with experimental data of H_s and H_c. The slope of $H_{c2}(t)$ at the transition temperature is $[dH_{c2}(t)/dt]_{t=1} = 84.4$.

In Fig. 6 the experimental ratio H_s/H_c vs $\kappa(t)$ is plotted together with the results of Park from his table of calculated values. The straight line is the ratio $H_{c3}/H_c = 2.392\,\kappa(t)$ (assuming the validity of SJdG's relation to extend to all temperatures). This line coincides, as it should, with the extrapolation of the results of Park to lower values of κ. As typical calculations of the ratio H_{c3}/H_c, we have plotted that of Hu and Korenman[34] for the case of specular reflection of the electrons from the surface and that of Luders[35] for the two cases of $P = 0.5$ and $P = 1$, where P is a parameter proportional to the diffuseness of the surface. The crossing of the experimental points from the curve of Park to the curve of H_{c3}/H_c is not contrary to his theoretical predictions and can be attributed to his wrong choice of H_{c3}, thus confirming the recent theoretical calculations[34,35] of H_{c3}. The value of κ at which the experimental points deviate from the curve of H_{c3}/H_c is taken to be $\kappa_c = 0.375$. Only if $\kappa < \kappa_c$ can H_{c3} be identified with the supercooling field. The fact that the characteristic κ of our sample was such as to display this region is fortuitous; however, the range of comparison of the possible experimental points with the theoretical calculations of H_{c3}/H_c is too small to allow a quantita-

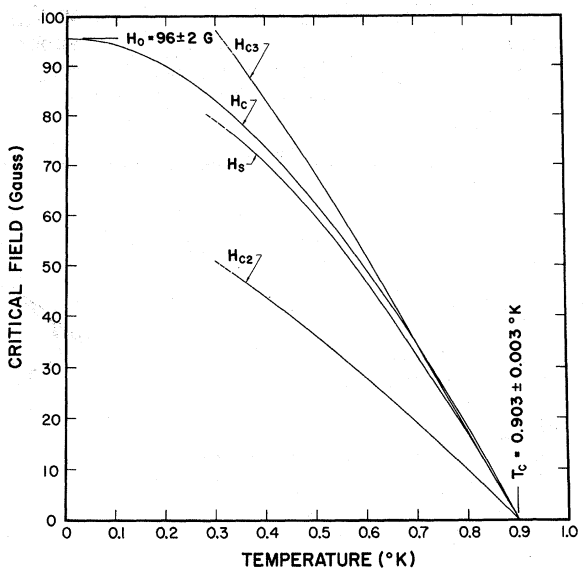

FIG. 5. Critical fields of molybdenum. H_c and H_s are measured experimentally. H_{c2} is calculated from H_c and κ according to the theory of Helfand and Werthamer (Ref. 41). H_{c3} is calculated from the expression of Hu and Korenman (Ref. 34).

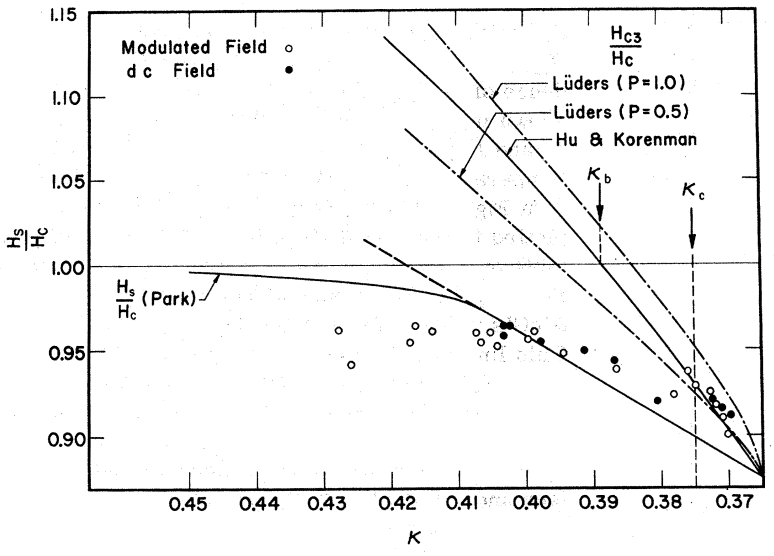

FIG. 6. Experimental ratio H_s/H_c vs κ of molybdenum. The extrapolated value of $\kappa(T_c)$ is 0.365 (see text). The experimental points fall on the curve of Hu and Korenman (Ref. 34) up to $\kappa_c = 0.375$ and deviate from it to follow the results of Park (Ref. 38) for $\kappa > \kappa_c$. The straight line is the ratio H_{c3}/H_c, assuming the validity of the SJdG relation (Ref. 32) at $T = T_c$ to be extended to lower temperatures (see text). The dash-dot lines are calculated from the results of Luders (Ref. 35) for the cases of $P = 0.5$ and $P = 1.0$, where P is a measure of the diffuseness of the surface.

tive comparison between the different theories. From Fig. 6 one can obtain $\kappa_b = 0.389$ at which H_{c3} changes from smaller to larger than H_c. At higher values of κ, i.e., $\kappa > \kappa_b$, the experimental points fall systematically below the calculated values of Park and show only a small tendency to approach the value $H_s/H_c = 1$ in the limit of large κ.

Thus, one can clearly distinguish three regions: firstly, $\kappa < \kappa_c$, where $H_s = H_{c3} < H_c$; secondly, $\kappa_c < \kappa < \kappa_b$, where $H_s < H_{c3} < H_c$; and, finally, $\kappa > \kappa_b$, where $H_s < H_c < H_{c3}$. These regions are shown in Fig. 5, where H_{c3} is plotted along with other critical fields of molybdenum vs temperature. In the region where the supercooling field is smaller than H_{c3}, a metastable surface sheath coexists with a supercooled normal bulk. It would be of interest to extend the results of the present work to lower values of κ and compare the supercooling field with the calculations of H_{c3}. The early work of Pinatti and Rorschach[22] on supercooling of molybdenum shows a decrease in κ by annealing. Unfortunately, the complete temperature dependence of their data was not available to determine whether it falls on the extension of the present data to lower values of κ.

B. Thermal Conductivity in Superconducting and Normal States

The temperature dependence of the thermal conductivity of molybdenum in the superconducting state K_s and in the normal state K_n is plotted in Fig. 7. K_s and K_n, below 1 °K, are also plotted in Fig. 8. The critical temperature T_c is estimated

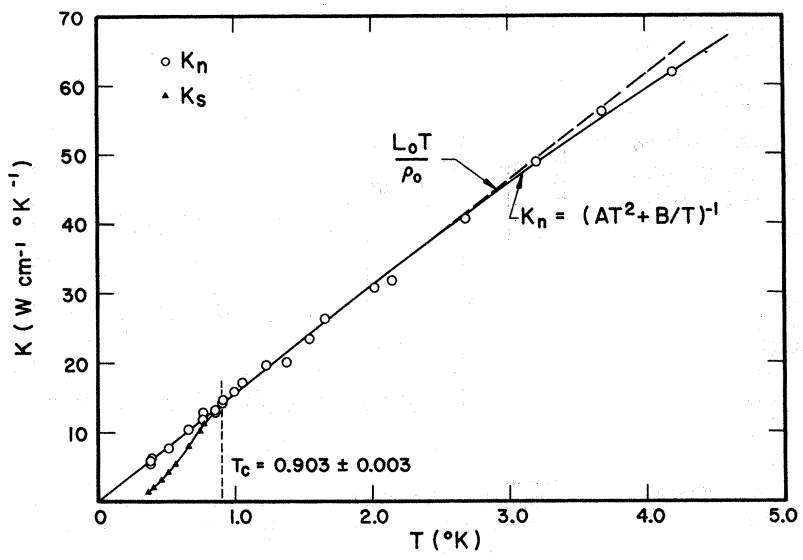

FIG. 7. Thermal conductivity of molybdenum in the normal and superconducting states. The solid line is a least-squares fit of the form $K_n = (AT^2 + B/T)^{-1}$ to the data, where $A = 5.13 \times 10^{-5}$ W^{-1} cm deg^{-1} and $B = 6.40 \times 10^{-2}$ W^{-1} cm deg^2. The dashed line is obtained from the residual electrical resistivity ρ_0 through the Wiedmann-Franz law $K_{en} = L_0 T/\rho_0$.

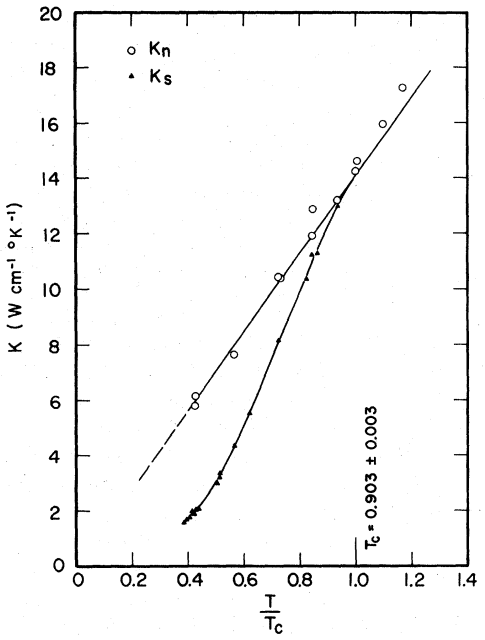

FIG. 8. Thermal conductivity of molybdenum in the normal and superconducting states below the transition temperature. The solid line through the normal points is a least-squares fit of the form $K_n = (AT^2 + B/T)^{-1}$ (see Fig. 7).

to be the same as that determined from the critical field measurements. The solid line passing through the normal points is a least-squares fit of the form $K_n = (AT^2 + B/T)^{-1}$ to the data, where $A = 5.13 \times 10^{-5}$ W^{-1} cm deg^{-1} and $B = 6.40 \times 10^{-2}$ W^{-1} cm deg^2. The straight dashed line which very nearly fits the data below 1 °K is obtained from the residual resistivity ρ_0 by assuming the validity of the Wiedemann-Franz relation $K_n = L_0 T/\rho_0$ ($\rho_0 = 1.58 \times 10^{-9}$ Ωcm, $K_n = 15.5T$ W cm^{-1} deg^{-1}). The tendency of the experimental data to fall below this line above the transition temperature is attributed to a small resistive component due to scattering of electrons by phonons. The analysis of the normal-state conductivity in terms of different scattering mechanisms has been made for a free-electron model.[42] The electronic thermal conductivity K_{en} at $T < \Theta/10$ (Θ is the Debye temperature) is given by

$$1/K_{en} = AT^2 + B/T\,, \qquad (1)$$

where $A = 95.3 N_a^{2/3}/K_\infty^2$ and $B = \rho_0/L_0$; N_a is defined as the effective number of conduction electrons per atom, K_∞ is the limiting value of the electronic thermal conductivity at high temperatures, ρ_0 is the residual electrical resistivity, and L_0 is the Lorentz number. The first term on the right-hand side of Eq. (1) represents the electronic thermal resistivity due to phonon scattering, and the second term represents the electronic thermal resistivity due to impurity scattering. Figure 9 shows the plot of T/K_n vs T^3. The straight line represents a least-squares fit to the data. The slope of the straight line gives the value of the constant $A = 5.13 \times 10^{-5}$ W^{-1} cm deg^{-1}. The intercept gives $B = 6.40 \times 10^{-2}$ W^{-1} cm deg^2, which differs by about 1% from the result obtained from the residual resistivity measurements. From the experimental value of A and using[21] $\Theta = 456$ °K and[43] $K_\infty = 0.8$ W cm^{-1} deg^{-1}, we derive an effective number of conduction electrons per atom ($N_a = 0.89$). The BRT theory[14] assumes elastic impurity scattering of the electrons in the calculations of the ratio K_{es}/K_{en}, where K_{es} and K_{en} are the electronic contributions to the thermal conductivity in the superconducting and normal states. Kadanoff and Martin[44] have calculated the ratio K_s/K_n taking into account electron-phonon interaction and impurity scattering. Their calculation involves a parameter $a = AT^3/B$, which is the ratio of the phonon scattering to the impurity scattering in the thermal resistivity. In the limit of predominance of impurity scattering, i.e., $a \simeq 0$, their result is identical with that of BRT. Using the experimental values of A and B, one finds $a \simeq 10^{-3} T^3$, and therefore the phonon contribution to the scattering below 1 °K is estimated to be, at most, 0.1% of the total thermal resistivity. This corresponds to the case of $a = 0$ in the theory of Martin and Kadanoff. Thus, the preponderance of the impurity scattering below 1 °K allows us to make a direct comparison of the temperature dependence of K_s/K_n to the theory of BRT. The predominance of the electronic contribution to the thermal conductivity of the sample is confirmed

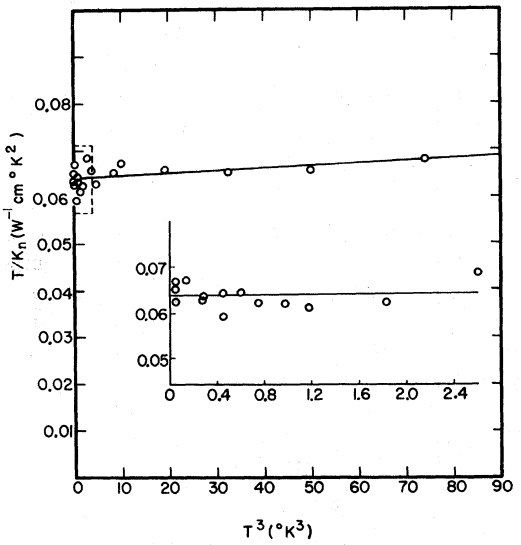

FIG. 9. Plot of T/K_n vs T^3. The straight line is a least-squares fit to determine the coefficients A and B in $1/K_n = AT^2 + B/T$ (see text).

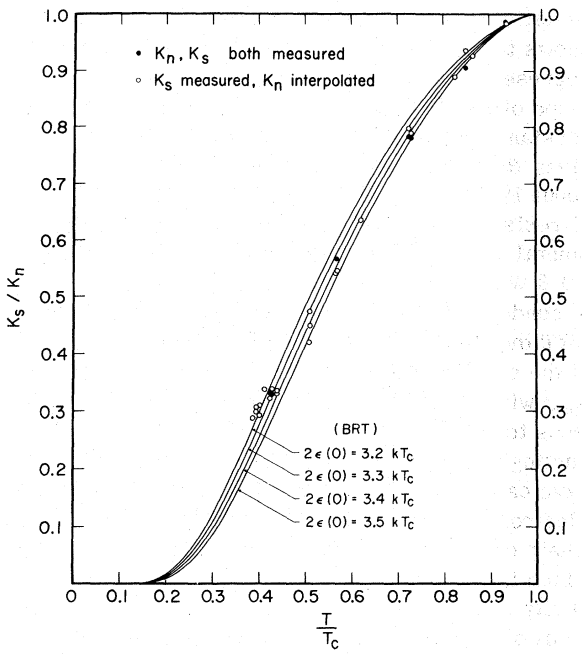

FIG. 10. Ratio of the superconducting to normal conductivities vs reduced temperature. The solid curves are the theoretical BRT ratios for different values of energy gap.

from its electrical- and thermal-conductivity measurements in high magnetic fields.[45] It was observed that the normal lattice conductivity K_{gn} was not more than 0.1% of the total conductivity K_n. It is also shown later in the text that the superconducting lattice conductivity K_{gs} does not exceed more than 3% of K_s. Therefore, $K_s/K_n \simeq K_{es}/K_{en}$ in the case of our sample. The BRT relation for the case of elastic impurity scattering of electrons is

$$K_{es}/K_{en} = [2F_1(-y) + 2y \ln(1+e^{-y}) + y^2(1+e^{y})^{-1}]/2F_1(0)\,, \qquad (2)$$

where $y = \epsilon(t)/kT = [\epsilon(t)/\epsilon(0)]\,[\epsilon(0)/kT_c]\,(1/t)$, $\epsilon(t)$ being the half-width of the energy gap at temperature T in the BCS theory. The temperature dependence of $\epsilon(t)/\epsilon(0)$ has been calculated by Mühlschlegel[31] based on the BCS theory and the term $F(-y)$ is given by the expression

$$F_n(-y) = \int_0^\infty \frac{z^n\,dz}{1+e^{z+y}}\,.$$

The experimental values of K_s/K_n vs reduced temperature are plotted in Fig. 10 together with that of BRT for several values of the energy gap. It is observed that the value of the energy gap $2\epsilon(0)/kT_c = 3.4 \pm 0.1$ agrees reasonably well with the experimental results for temperatures $T > 0.5T_c$. This value coincides with the one we obtain from the critical field measurements. At lower temperatures, however, there is a definite tendency of the experimental points to deviate from the BRT relation and this deviation is more than the probable experimental errors.

In view of the over-all agreement of the experimental ratio K_s/K_n with the result of BRT for K_{es}/K_{en}, and the close agreement of the critical field measurements with the theory of BCS, one may choose to give an immediate and self-contained explanation. Superconductivity in molybdenum is the same as that in the nontransition metals and the deviation of the experimental data from the BRT curve, at lower temperatures, is due to the increase of the lattice contribution to the thermal conductivity state. From BRT's theory, K_{gs} increases with decreasing temperature and is proportional to T^{-3}. In fact, Engelhardt *et al.*[5] have argued that the s-d interaction in molybdenum, owing to the intrinsic stability of a half-filled d shell and high lattice stability for a $d^5 s^1$ configuration, is *small*, and the s electrons, as in nontransition elements, are the major contributors to the superconductivity. This argument is supported by the T^5 dependence of the resistivity of molybdenum[46] in the normal state which is attributed to the scattering of the s electrons by phonons into s states.[47] However, the discussion below will show that the assumption of nontransitionlike superconductivity in molybdenum and the complete absence of s-d interaction, which is inherent in that assumption, has several shortcomings.

s-d Interaction. The energy-gap parameter obtained by fitting the experimental data to the theory of BRT is larger[48] than the value determined by ultrasonic attenuation[18] in the study of the anisotropy of the energy gap in molybdenum as shown in Table I. Moreover, a consequence of fitting the experimental data with a BRT curve is to attribute the deviations from the curve, at low temperatures, to the lattice contribution to the thermal conductivity. This deviation, as seen in Fig. 10, amounts to a 15% increase over the electronic conductivity in the superconducting state at temperature $T = 0.4T_c$. This would indicate that the lattice contribution is about $K_{gs} \simeq 0.255\ \mathrm{W\,cm^{-1}\,deg^{-1}}$. It can be shown,[45] using magnetoresistance measurements, that such high lattice conductivity in the superconducting state leads to an unreasonably high ratio $K_{gs}/K_{gn} \simeq 400$ since K_{gn}, at this temperature, is estimated to be only $0.0006\ \mathrm{W\,cm^{-1}\,deg^{-1}}$. Comparison of this result with the calculations of BRT, for the case of lattice conductivity limited by electron scattering, shows that it is approximately 5 times larger than their prediction. Thus, a generous estimate of the lattice contribution K_{gs} to the

thermal conductivity K_s does not, at $T = 0.4T_c$, exceed more than 3% of the total conductivity. Therefore, the source of the deviation of the experimental data of K_{es}/K_{en} from the BRT curve must lie elsewhere.

It is well known that the transport properties of transition metals, both in the normal and superconducting states, should be influenced by the presence of a narrow energy band with high density of states, i.e., the d band. The role of the d band in conduction seems to be mostly that of providing a number of alternative states in which s electrons can be scattered. Following the initial work of Suhl *et al.*,[8] who proposed that in transition elements the superconducting state may be characterized by a two-band structure with contributions arising from interband s-d scattering, Vasudevan and Sung[15] extended the BRT calculation on thermal conductivity due to impurity scattering to the two-band model.

The basic feature of these results is that the added resistance due to interband scattering is prominent only close to T_c. Qualitatively, for the transition metals, this means that when one fits experimental results to the BRT curve, one should expect the points close to T_c to fall below the theoretical curve and only points at lower temperatures should be expected to agree with BRT and to yield a reliable value of the energy gap.

From this point of view, we reinterpret Fig. 10 as follows: Fitting the lowest group of points to BRT yields an energy gap $2\epsilon(0)/kT_c = 3.2 \pm 0.1$ while the shift of the points at higher temperatures gives an indication of the effect of allowing interband transitions due to impurity scattering.[49] An extension of the data to lower temperatures would be needed to make this argument more than qualitative. The disagreement between the above value of the energy gap and the results of the specific-heat measurements[21] and our critical field measurements is believed to be due to the anisotropy of the energy gap.[48]

There exists corroborating evidence in the experimental results obtained in niobium by Wasim and Zebouni.[29] The straight fits with BRT curves presented in their work yield an energy gap of 3.96. This result is higher than most previous experimental determinations, especially those made by tunneling.

We now think that the niobium data, taking into account the influence of impurity scattering in the two-band model, should be fitted with a BRT curve of approximately $2\epsilon(0)/kT_c \simeq 3.8$. The situation in the niobium case is evidently complicated by the sharp rise of lattice conductivity at lower temperatures.

In conclusion, we are suggesting that results of thermal conductivity in the superconducting state of transition metals, when they are fitted with a BRT curve, yield only an upper limit of the value of the energy gap. The situation is quite delicate, since not only is there added scattering close to T_c, but there also is added conductivity due to the increase in the lattice contribution at the lower end of the temperature range.

V. CONCLUSION

The existence of a supercooling critical field H_{s}, separate and distinct from the surface nucleation field H_{c3}, is established for values of κ larger than κ_c. This confirms that the superconducting surface sheath can exist simultaneously with a supercooled normal bulk. The results of the thermal-conductivity measurements suggest that caution should be exerted in the comparison to BRT theory because of the possibility of reduced conductivity close to T_c due to s-d scattering. This consideration makes the determination of the energy gap by thermal-conductivity measurements rather uncertain.

ACKNOWLEDGMENTS

The authors wish to express their appreciation for the help provided by Dr. S. Wasim and Dr. K. Tanaka. They are also grateful to Professor C. G. Grenier for his advice and stimulating discussions. One of the authors (A. W.) wishes to acknowledge the Dr. Charles E. Coates Memorial Fund of the L. S. U. Foundation, donated by George H. Coates, for assistance in the publication of this manuscript.

---

†This work was supported by the U. S. Atomic Energy Commission under Contract No. AT-(40-1)-3087 and is AEC Report No. ORO-3087-46.

[1]B. T. Matthias, T. H. Geballe, E. Corenzwit, and G. W. Hull, Jr., Phys. Rev. 129, 1025 (1963); G. E. Devlin and E. Corenzwit, *ibid.* 120, 1964 (1960); T. H. Geballe, B. T. Matthias, G. W. Hull, Jr., and E. Corenzwit, Phys. Rev. Letters 6, 275 (1961); R. D. Fowler, J. D. G. Lindsay, R. W. White, H. H. Hill, and B. T. Matthias, *ibid.* 19, 892 (1967); H. H. Hill, W. White, J. D. G. Lindsay, R. D. Fowler, and B. T. Matthias, Phys. Rev. 163, 356 (1967); E. Maxwell, M. Strongin, and T. B. Reed, *ibid.* 166, 457 (1968).

[2]E. Bucher and J. L. Olsen, in *Proceedings of the Eighth International Conference on Low-Temperature Physics, London*, 1962, edited by R. O. Davies (Butterworth, Washington, D. C., 1963); J. L. Olsen, E. Bucher, M. Levy, J. Muller, E. Corenzwit, and T. H. Geballe, Rev. Mod. Phys. 36, 168 (1964); W. E. Gardner and T. F. Smith, Phys. Rev. 144, 233 (1966); C. W. Chu, T. F. Smith, and W. E. Gardner, Phys. Rev. Letters 20, 198 (1968); C. W. Chu, W. E. Gardner, and T. F. Smith, Phys. Letters 26A, 627 (1968).

[3]J. K. Hulm, R. D. Blaugher, T. H. Geballe, and

B. T. Matthias, Phys. Rev. Letters 7, 302 (1961).

[4]A. M. Clogston, B. T. Matthias, M. Peters, H. J. Williams, E. Corenzwit, and R. C. Sherwood, Phys. Rev. 125, 541 (1962); B. R. Coles, Phil. Mag. 8, 335 (1963).

[5]J. J. Engelhardt, G. W. Webb, and B. T. Matthias, Science 155, 191 (1967).

[6]B. T. Matthias, in *Proceedings of the Eighth International Conference on Low-Temperature Physics, London*, 1962, edited by R. O. Davis (Butterworth, Washington, D.C., 1963); B. T. Matthias, T. H. Geballe, and V. B. Compton, Rev. Mod. Phys. 35, 1 (1963); T. H. Geballe, *ibid.* 36, 134 (1964); R. C. Hamilton and M. Anthony Jensen, Phys. Rev. Letters 11, 205 (1963).

[7]J. Bardeen, L. N. Cooper, and J. R. Schrieffer, Phys. Rev. 108, 1175 (1957).

[8]H. Suhl, B. T. Matthias, and L. R. Walker, Phys. Rev. Letters 3, 552 (1959).

[9]J. W. Garland, Jr., Phys. Rev. Letters 11, 111 (1963).

[10]P. W. Anderson, J. Phys. Chem. Solids 11, 26 (1959).

[11]J. W. Garland, Jr., Phys. Rev. Letters 11, 114 (1963).

[12]G. Gusman, J. Phys. Chem. Solids 28, 2327 (1967).

[13]P. Morel and P. W. Anderson, Phys. Rev. 125, 1263 (1962); W. L. McMillan, *ibid.* 167, 331 (1968).

[14]J. Bardeen, G. Richayzen, and L. Teword, Phys. Rev. 113, 982 (1959).

[15]R. Vasudevan and C. C. Sung, Phys. Rev. 144, 237 (1966).

[16]T. H. Geballe, B. T. Matthias, E. Corenzwit, and G. W. Hull, Jr., Phys. Rev. Letters 8, 313 (1962).

[17]N. H. Horwitz and H. V. Bohm, Phys. Rev. Letters 9, 313 (1962).

[18]C. K. Jones and J. A. Rayne, Phys. Letters 26A, 75 (1967).

[19]R. A. Hein, J. W. Gibson, M. R. Pablo, and R. D. Blaugher, Phys. Rev. 129, 136 (1963).

[20]G. D'yakov and A. D. Shets, Zh. Eksperim. i Teor. Fiz. 49, 1091 (1965) [Sov. Phys. JETP 22, 759 (1966)].

[21]D. C. Rorer, D. G. Onn, and H. Meyer, Phys. Rev. 138, A1661 (1965).

[22]R. G. Mallon and H. E. Rorschach, Jr., Phys. Rev. 158, 418 (1967); D. G. Pinatti, Ph.D. thesis (Rice University, Houston, Tex., 1969) (unpublished).

[23]H. A. Reich and R. L. Garwin, Rev. Sci. Instr. 30, 7 (1959).

[24]A. Waleh and L. Edelen (unpublished).

[25]Supercon T48B was purchased from Supercon Division of Norton Co. (formerly National Research Corp.).

[26]S. G. Sydoriak and R. H. Sherman, J. Res. Natl. Bur. Std. (U. S.) A68, 547 (1964); T. R. Roberts and S. G. Sydoriak, Phys. Rev. 102, 304 (1956).

[27]R. S. Blewer, N. H. Zebouni, and C. G. Grenier, Phys. Rev. 174, 700 (1968).

[28]S. Cunsolo, M. Santini, and M. Vicentini-Missoni, Cryogenics 5, 168 (1965); P. P. Craig, *ibid.* 6, 112 (1966).

[29]S. M. Wasim and N. H. Zebouni, Phys. Rev. 187, 539 (1969).

[30]$H_c(T) = 95.6 - 144.4\,T^2 + 51.8\,T^4 - 22.6\,T^6$, $H_s(T) = 89.7 - 120.3\,T^2 - 0.5\,T^4 + 16.7\,T^6$.

[31]B. Mühlschlegel, Z. Physik 155, 313 (1959).

[32]D. Saint-James and P. G. de Gennes, Phys. Letters 7, 306 (1963).

[33]V. L. Ginzburg and L. D. Landau, Zh. Eksperim. i Teor. Fiz. 20, 1064 (1950).

[34]C. R. Hu and V. Korenman, Phys. Rev. 178, 684 (1969); 185, 672 (1969).

[35]G. Luders, Z. Physik 202, 8 (1967).

[36]C. Ebner, Solid State Commun. 7, 1207 (1969).

[37]J. Feder, Solid State Commun. 5, 299 (1967).

[38]J. G. Park, Solid State Commun. 5, 645 (1967).

[39]J. P. McEvoy, D. P. Jones, and J. G. Park, Solid State Commun. 5, 641 (1967).

[40]L. P. Gor'kov, Zh. Eksperim. i Teor. Fiz. 37, 833 (1959) [Sov. Phys. JETP 10, 593 (1960)].

[41]E. Helfand and N. R. Werthamer, Phys. Rev. 147, 288 (1966).

[42]R. E. B. Makinson, Proc. Cambridge Phil. Soc. 34, 474 (1938).

[43]C. Y. Ho, R. W. Powell, and P. E. Liley, *Thermal Conductivity of Selected Materials*, Part 2, NSRDS-NBS No. 16 (U.S. Department of Commerce, U. S. GPO, Washington, D. C., 1968).

[44]L. P. Kadanoff and P. C. Martin, Phys. Rev. 124, 670 (1961).

[45]In the presence of a very high magnetic field, the electronic contributions to the thermal conductivity will be suppressed enough to make the observation of the lattice contribution possible. Then one can write the following:

$$\frac{K_n(H)}{K_n(0)} = \frac{K_{en}(H)+K_{gn}}{K_{en}(0)+K_{gn}} \simeq \frac{K_{en}(H)+K_{gn}}{K_{en}(0)},$$

and from the Wiedemann-Franz relation it follows that

$$\frac{K_{gn}}{K_n(0)} \simeq \frac{K_n(H)}{K_n(0)} - \frac{\rho_0(0)}{\rho_0(H)}.$$

From the thermal and electrical conductivity measurements of the sample between 1.2–4.2 °K, in a transverse magnetic field of about 10^4G, $K_n(0)/K_n(H) \simeq 210$ and $\rho_0(H)/\rho_0(0) \simeq 270$; therefore, $K_{gn}/K_n \simeq 10^{-3}$.

[46]N. V. Vol'kenshteyn, Ye. P. Romanov, L. S. Starostina, and V. Ye Startsev, Phys. Metals Mettallog. USSR 17, 152 (1964); G. K. White and S. B. Woods, Phil. Trans. Roy. Soc. London A251, 273 (1959).

[47]F. Bloch, Z. Physik 59, 208 (1930).

[48]The thermal conductivity of the sample was measured along a direction very close to [111]. One expects to observe the effect of the anisotropy of energy gap in the thermal conductivity of a pure sample, while the specific-heat and thermodynamic critical field measurements would only yield a mean value of the energy gap.

[49]An alternative explanation for the behavior of the thermal conductivity of molybdenum is to assume a partial contribution from the *s-d* interaction. Thus, one may propose that the superconducting state in the transition metals should be characterized by a two-band structure in which the contributions from the interband scattering depend on a parameter determined from the lattice stability and the electronic configuration. Such a model will be consistent with the observations on niobium and Tungsten (see Ref. 5).